Debottlenecking of an In Vitro Enzyme Cascade Using a Combined Model- and Experiment-Based Approach

Regine Siedentop, Marlon Dziennus, Stephan Lütz, and Katrin Rosenthal*

DOI: 10.1002/cite.202200170

Supporting Information available online

Dedicated to Prof. Dr. Christian Wandrey on the occasion of his 80th birthday

Designing a feasible in vitro enzyme cascade is a challenging task that is often preceded by optimization steps. Computational methods can increase the efficiency of the optimization process by providing a deeper insight into the system. In this study, bottlenecks of a farnesyl pyrophosphate-producing in vitro enzyme cascade were determined by a combination of in silico modeling and wet-lab experiments. ATP and the precursor-isomerizing enzyme isopentenyl diphosphate δ-isomerase were identified as limitations of the in vitro enzyme cascade.

Keywords: Biocatalysis, Enzyme cascades, In vitro biotransformations, Kinetic models, Terpenes

Received: August 24, 2022; *revised:* December 12, 2022; *accepted:* January 18, 2023

1 Introduction

The use of whole-cell biocatalysis and isolated enzymes for the synthesis of valuable compounds becomes increasingly important. Biocatalysis offers many advantages such as greener processes and high regio-, stereo-, and enantioselectivity [1]. The combination of several isolated enzymes and hence sequential reactions in one pot is called in vitro enzyme cascade. This enables the use of simple starting materials, reduces the need for the isolation of intermediates, and shifts the equilibrium towards product side. New synthesis routes were developed for complex molecules [2] and by the usage of in vitro enzyme cascades, the product titer can exceed their cellular counterpart [3]. Nevertheless, working with such a system is challenging, since many enzymes have to be adapted to the same reaction conditions. In addition, cofactor regeneration systems often have to be included [4]. Therefore, multi-enzyme reactions usually do not reach their full performance directly but have to be optimized to increase their performance [5]. This can be a challenging and laborious task, especially for complex systems. In silico models of enzyme cascades can support the identification of parameters that have an impact on the performance by providing deeper insights. As a result, in silico models can reduce the amount of wet-lab experiments required for optimization [6–8].

Here, a farnesyl pyrophosphate (FPP)-producing enzyme cascade previously reported by Dirkmann et al. was optimized (Fig. 1) [9]. This cascade suffers from low yields, high adenosine triphosphate (ATP) consumption, and many possible interactions between substrates, intermediates, and enzymes due to many catalytic steps. The goal of the optimization was the identification of the limiting steps and subsequent adaptation of the enzyme cascade. A combination of in silico modeling and wet-lab experiments was chosen for this task. A kinetic model of the ten-enzyme cascade was developed in COPASI (Complex Pathway Simulator), a software application for the simulation and analysis of biological processes [10]. Using this model, bottlenecks were identified, and wet-lab experiments validated their importance for the cascade's performance.

[1]Regine Siedentop https://orcid.org/0000-0002-8514-9538,
[1]Marlon Dziennus,
[1]Prof. Dr. Stephan Lütz https://orcid.org/0000-0001-8534-0554,
[2]Prof. Dr.-Ing. Katrin Rosenthal
https://orcid.org/0000-0002-6176-6224
(katrin.rosenthal@tu-dortmund.de)
[1]TU Dortmund University, Chair for Bioprocess Engineering, Department of Biochemical and Chemical Engineering, Emil-Figge-Straße 66, 44227 Dortmund, Germany.
[2]Constructor University, Department of Life Sciences and Chemistry, Campus Ring 1, 28759 Bremen, Germany.

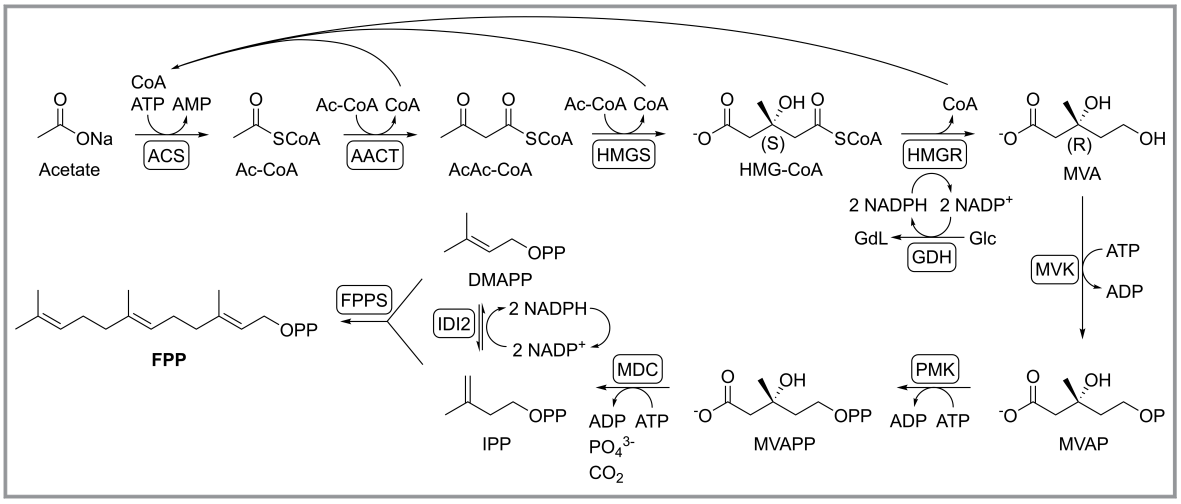

Figure 1. FPP-producing in vitro enzyme cascade, starting with acetate and following the steps of the mevalonate pathway [9]. Nine anabolic steps with ten enzymes are involved, while the cofactors CoA and NAPDH get recycled. The substrates acetate, ATP, and glucose have to be added in stoichiometric amounts. AACT, acetoacetyl-CoA synthase; AcAc-CoA, acetoacetyl-coenzyme A; Ac-CoA, acetyl-coenzyme A; ACS, acetyl-CoA synthetase; ADP, adenosine diphosphate; AMP, adenosine monophosphate; ATP, adenosine triphosphate; CoA, coenzyme A; DMAPP, dimethylallyl diphosphate; FPPS, (2*E*,6*E*)-farnesyl diphosphate synthase; GDH, glucose dehydrogenase; GDL, glucono δ-lactone; Glc, glucose; HMG-CoA, 3-hydroxy-3-methylglutaryl-CoA; HMGR, 3-hydroxy-3-methylglutaryl-coenzyme A reductase; HMGS, 3-hydroxy-3-methylglutaryl-CoA synthase; IDI, isopentenyl diphosphate δ-isomerase; IPP, isopentenyl pyrophosphate; MDC, diphosphomevalonate decarboxylase; MVK, mevalonate kinase; NADP(H), nicotinamide adenine dinucleotide phosphate; PMK, phosphomevalonate kinase.

2 Experimental

2.1 Construction of the Kinetic Model

The kinetic model for the FPP-producing cascade was constructed in COPASI (v4.30, http://copasi.org/) [11]. Equations were built on the basis of the reaction's rate law (Eq. (1))

$$R = \frac{U_{\max}}{1000} \frac{\frac{AB - \frac{PQ}{K_{eq}}}{K_A K_B}}{\left(1 + \frac{A}{K_A}\right)\left(1 + \frac{B}{K_B}\right) + \left(1 + \frac{P}{K_P}\right)\left(1 + \frac{Q}{K_Q}\right) - 1} \quad (1)$$

with R as reaction rate, A and B as substrate concentration, and P and Q as product concentration. K_x is the Michaelis-Menten constant of compound x, which was obtained from the databank BRENDA for all enzymes (Tab. S1 in the Supporting Information). U_{max} defines the enzyme activity and K_{eq} was calculated by Eq. (2). If necessary, K_{eq} was set to a value at which the reaction would take no longer than 24 h, a value chosen from experience (Tab. S1).

$$K_{eq} = K_{eq,0} \frac{K_P K_Q}{K_A K_B} \quad (2)$$

$K_{eq,0}$ was set to 2 to present more substrate ($K_{eq} > 1$) than product at the beginning of the respective reaction. For irreversible reactions, an IF-query (Eq. (3)) was implemented to suppress a reverse reaction.

$$\text{IF: } R < 0, \quad \text{then } R = 0, \quad \text{else } R = R \quad (3)$$

The data that the model was built on was obtained from literature describing the kinetic properties of the enzymes. If such data were not available, the properties of homologous enzymes were used (Tab. S1). Parameter scans were performed in COPASI by varying the enzyme concentrations and thus the reaction rates, with the objective function of producing the highest possible FPP yields. No limits were set for the enzyme concentrations, but they were varied until the optimum was reached. Product concentrations were evaluated if the reaction was in equilibrium or it reached 24 h.

2.2 Materials

The chemicals were purchased from Santa Cruz Biotechnology (Santa Cruz Biotechnology, Inc. Dallas, Texas, USA), Roth (Carl Roth, Karlsruhe, Germany), VWR (VWR international GmbH, Darmstadt, Germany), ThermoFisher (ThermoFisher Scientific, Waltham, MA, USA), Merck (Merck KGaA, Darmstadt, Germany), and AppliChem (AppliChem GmbH, Darmstadt, Germany).

2.3 Enzyme Preparation

Instructions of enzyme preparation for FPP synthesis were taken from Dirkmann et al. [9]. PPKs were prepared according to Becker et al. [12].

2.4 FPP Synthesis

FPP synthesis was performed in 1.5 mL Eppendorf tubes. Tab. S3 shows the composition of the assays in 350 µL cascade buffer (100 mM TrisHCl, 150 mM NaCl, 10 % glycerol, 20 mM $MgCl_2$, pH 7.5). The reactions were performed at 30 °C in a multirotator rotating with 30 rpm for 24 h. Samples were prepared according to Dirkmann et al. [9].

2.5 Analytics

FPP was analyzed using a liquid chromatography-mass spectrometry (LC-MS; 1260 Infinity II LC system combined with 6120 Quadrupole MS (Agilent, Santa Clara, CA, US)) system with a NUCLEODUR C18 Gravity column (3 µm, 150×2 mm, Macherey-Nagel GmbH & Co. KG, Düren, Germany). The flow rate was 0.4 mL min^{-1} and the column oven was set to 35 °C. The injection volume was 3 µL. The following gradient of 10 mM NH_4Ac, pH 9.2 (mobile phase A) and acetonitrile (mobile phase B) was used: 0–1.5 min: 5 % B, 1.5–6 min: 5–60 % B, 6–8.5 min: 60–80 % B, 8.5–14.5 min: 80 % B, 14.5–15 min: 80–95 % B, 15–20 min: 95 % B, 20–21 min: 95–5 % B, 21–25 min: 5 % B. The MS measurement was performed in negative mode and the electron spray ionization (ESI) was set to the following parameters: drying gas temperature: 350 °C, nebulizer pressure: 35 psig, drying gas flow: 12 L min^{-1}, capillary voltage: 3500 V. Analytes were detected in SIM mode with *m*/*z* of 301–301.1 (for farnesyl phosphate), 381.1–381.2, and 763.2–763.3 (for monomeric and dimeric FPP, respectively).

3 Results and Discussion

3.1 Development of a Kinetic Model for In Vitro FPP Synthesis

Even though the general feasibility of synthesizing FPP from acetate was demonstrated, several challenges exist for the production of FPP using an enzyme cascade starting from acetate: FPP is produced in low yields, the mevalonic pathway is strictly regulated, and ATP has to be added in large quantities because 18 molecules are needed for each molecule of FPP [9, 13]. The low yield with 4 mmol L^{-1} FPP of 170 mmol L^{-1} acetate can be due to low substrate conversion, accumulation or depletion of intermediates, or unfavorable equilibria [9]. Improving the performance using only experimental methods is a challenging task because of the complexity of the cascade with ten involved enzymes. The quantification of all intermediates is difficult and the interactions of all intermediates and enzymes with each other are hard to monitor experimentally. Therefore, a computer model was developed for the optimization of the FPP-producing cascade by monitoring the intermediate levels for every time point and visualize relations between individual reaction steps using COPASI. With this approach, a better understanding of the fundamental features of the cascade and the identification of potential bottlenecks to increase the product concentration was expected.

For the development of the kinetic model, corresponding data such as U_{max} and K_M were taken from the BRENDA databank or were adapted from literature [13]. Values of enzyme homologs were taken if no other data were available and values for the equilibrium constants were either calculated or adjusted manually (Tab. S1). Finally, a mechanistic model of the cascade was created based on published experimental data [9] and time courses of the reaction were simulated (Fig. 2). Since the optimization of the final product concentration was of particular interest, considerations about the reaction rates were not included for further simulations.

The developed model revealed that ATP is a limiting component for FPP synthesis (Fig. 2). The cofactor was depleted before acetate was fully consumed and the intermediates mevalonate (MVA), mevalonate phosphate (MVAP), mevalonate pyrophosphate (MVAPP), which serve as substrates in ATP-dependent reactions, accumulated. Stoichiometric limitations were hence the main bottleneck, since for every molecule of acetate, two molecules of ATP are needed.

The reference cascade of the simulations was reenacted under the same conditions in wet-lab experiments in our laboratory (Tab. S3). However, the produced FPP concentration was too low for quantification. Therefore, we investigated the influence of an increased ATP supply on the cascade performance.

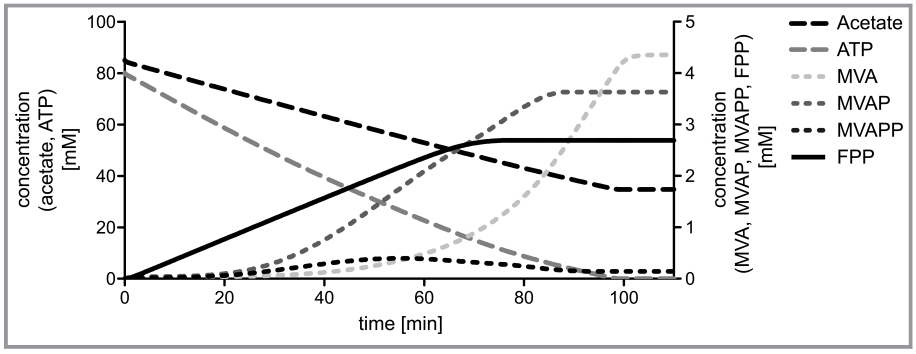

Figure 2. Simulated time course of ATP, ATP-dependent intermediates (mevalonate (MVA), mevalonate phosphate (MVAP), mevalonate pyrophosphate (MVAPP)), and the product of the FPP-producing cascade.

3.2 The Influence of Different ATP Supplies

To investigate the observed ATP limitation, two additional simulations were performed in which either ATP was added stoichiometrically or ATP was regenerated in situ.

The model was adjusted to a stoichiometric ATP concentration from 80 mM to 170 mM in relation to acetate with 85 mM. This ratio resulted in complete acetate conversion, as shown by the simulations (Fig. 3A). Furthermore, ATP was still present when FPP production stagnated and was thus no longer the limiting component. Investigating the amounts of the ATP-dependent intermediates showed an accumulation of MVA, MVAP, and MVAPP, even though enough ATP is present. This leads to the conclusion, that the equilibria of these reactions are unfavorable for FPP production. One way to pull the equilibria towards their product side is to remove coproducts such as AMP and ADP by their regeneration to ATP.

Therefore, an enzymatic ATP regeneration system was considered. This approach also gives an economic advantage of a cascade without any stoichiometric addition of often expensive cofactors. Here, polyphosphate kinases (PPKs) were included in the simulated cascade to phosphorylate the nucleotides using polyphosphate (PolyP) as phosphate donor, which is an established system for ATP regeneration [12, 14]. In the time courses of this approach, the initial amount of 20 mM ATP was rapidly consumed (Fig. 3B). Subsequently, acetate continued to be consumed and FPP was formed, which can be attributed to the regeneration of AMP and ADP into ATP. Furthermore, the ATP-dependent reactions were no longer limiting as acetate and the intermediates MVA, MVAP, and MVAPP diminished towards the end of the reaction (Fig. 3B).

Both simulations demonstrated that the achievable FPP concentrations can be increased by either supplying higher amounts of ATP or regenerating ATP (Tab. S2). Interestingly, regeneration of the cofactor led to significantly higher product concentrations compared to stoichiometric ATP addition (reference without adapted ATP supply: 2.7 mM FPP; stoichiometric ATP addition: 5.2 mM FPP; in situ regeneration of ATP: 8.8 mM FPP). However, wet-lab experiments conducted under the suggested conditions were not successful, and again FPP was not quantifiable. Since there can be other limitations or inhibitions in the cascade that are not overcome by providing ATP in stoichiometric amounts or using an ATP regeneration system, further regulating parameters of the cascade were considered.

3.3 Isomerization of IPP and DMAPP

The substrates of the final enzyme of the cascade, farnesyl diphosphate synthase (FPPS), are isopentenyl pyrophosphate (IPP) and dimethylallyl diphosphate (DMAPP). IPP and DMAPP are isomerized by the enzyme isopentenyl diphosphate δ-isomerase type 2 (IDI2). For the production of FPP, two molecules of IPP and one molecule of DMAPP are required. However, the investigation of the simulated time courses of the intermediates revealed an unfavorable equilibrium of the isomers IPP and DMAPP (Fig. 3). As can be seen in Fig. 3, the equilibrium of the isomerization is on the DMAPP side and only small amounts of IPP remain present, making further synthesis of FPP impossible. To overcome this limitation, other IDI variants with different catalytic properties were searched. There are two evolutionary distinct forms of this enzyme, type I (IDI1) and type II (IDI2), which differ in their reaction mechanism. IDI1 enzymes contain a zinc ion in their active side and IDI2 on the other hand is a flavoprotein that needs additional NADPH as a reducing agent [15]. In the simu-

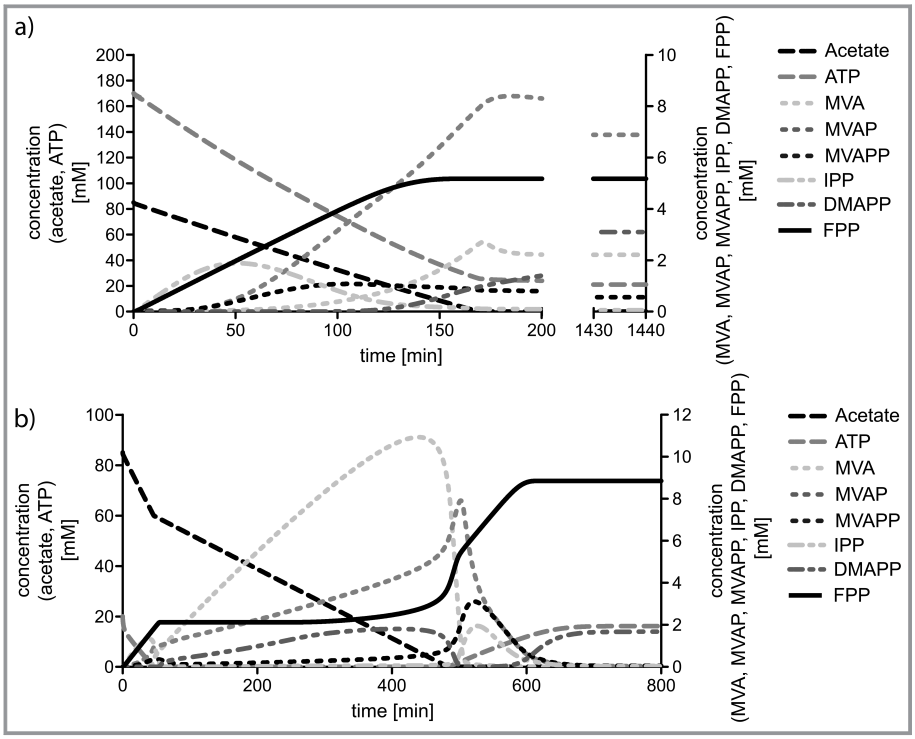

Figure 3. A) Simulated time course of ATP, ATP-dependent intermediates (MVA, MVAP, MVAPP), IDI-dependent molecules (IPP and DMAPP), and the product of the FPP-producing cascade with stoichiometric ATP amounts. The yield of FPP amounts to 55 %. B) Simulated time course of ATP, ATP-dependent intermediates, IDI-dependent molecules, and the product of the FPP-producing cascade with polyphosphate kinases to regenerate ATP.

lations and experiments, the IDI2 enzyme from *Thermus thermophilus* was used. For further investigations, three IDI1 mutant enzymes of *Escherichia coli*, R51K, K55A, and R83K, were considered and compared to the IDI2 enzyme [16]. The kinetics and structure of these three variants with single amino acid mutations were already described in literature. They had different catalytic properties with higher K_M values than the IDI2 variant and different specific activities (Tab. 1).

The simulations did not show significantly higher yields for the IDI mutations compared to the reference cascade (Tab. S2). However, the wet-lab validation of these findings discovered a different effect. All cascades, which contained the IDI1 variants produced quantifiable FPP concentrations. The IDI1 mutant with the highest FPP concentration was R83K with 129 µM FPP, followed by K55A with 79 µM FPP, and R51K with 3 µM FPP. Here, the mutation with the lowest substrate affinity and lowest reaction rate shows the lowest FPP concentration and the mutant with the highest substrate affinity and the highest reaction rate shows the highest FPP concentration. Thus, the last step of the cascade seems to have a decisive influence on the FPP production. By using IDI variants with a higher activity and affinity, the final product concentration can be significantly increased.

Still, higher terpene concentrations have been achieved in other systems, such as pinene from glucose in an enzymatic in vitro system or limonene production in *Escherichia coli* [13, 18]. But even though our final FPP concentrations were low, the combination of simulations and experiments led to a successful identification of bottlenecks of the FPP-producing cascade.

4 Conclusion

The interest in in vitro enzyme cascades has increased in recent decades and more and more attempts on cascade assemblies are performed [19]. Applications cover a broad field from the synthesis of complex high value compounds such as natural products or active pharmaceutical ingredients to bulk chemicals. The complex task of making such an enzyme cascade economically feasible makes optimization approaches increasingly relevant. As shown in this study, the combination of in silico and wet-lab experiments can reduce the amount of laborious work for an optimization. Kinetic simulations of the cascade can be performed and valuable information can be gained, which in turn can give indications of possible improvements. However, effects such as different reaction conditions, protein-protein interactions, or unknown inhibiting and activating influences can hardly be modeled. Therefore, wet-lab experiments have to validate the obtained information. Prior modeling reduces the workload, as simulations give hints to the right direction. This linkage enables targeted and straightforward optimization of in vitro enzyme cascades.

Supporting Information

Supporting Information for this article can be found under DOI: https://doi.org/10.1002/cite.202200170. This section includes additional references to primary literature relevant for this research [20–28].

We kindly thank Frank Schulz for providing the plasmids for the FPP-producing enzymes and for scientific discussion. This research was funded by Deutsche Forschungsgemeinschaft (DFG) under the priority programme SPP 2240 "eBiotech" (Bioelectrochemical and engineering fundamentals to establish electrobiotechnology for biosynthesis – Power to value-added products) (grant agreement No 445751305). Open access funding enabled and organized by Projekt DEAL.

Symbols used

K_{eq}	[–]	equilibrium constant
K_M	[mM]	Michaelis-Menten constant
K_x	[mM]	Michaelis-Menten constant of compound *x*
R	[mM s^{-1}]	reaction rate
U_{max}	[mmol s^{-1}]	enzyme activity

Abbreviations

AACT	acetoacetyl-CoA synthase
AcAc-CoA	acetoacetyl-coenzyme A

Table 1. Overview of the IDI variants, their kinetic properties, and the produced FPP concentrations using these variants in enzyme cascade wet-lab experiments. n.a., not available; n.d., not detected.

IDI variant	K_M [µM]	Specific activity [U mg^{-1}]	FPP concentration [µM]
IDI2 (reference cascade)	0.0056 [17]	n.a.	n.d.
IDI1 R51K	18.5 ± 2.0 [16]	5.4 ± 0.6 [16]	3 ± 1
IDI1 K55A	14.0 ± 1.9 [16]	83.4 ± 2.4 [16]	79 ± 22
IDI1 R83K	3.0 ± 0.5 [16]	132 ± 9 [16]	129 ± 5

Ac-CoA	acetyl-coenzyme A
ACS	acetyl-CoA synthetase
ADP	adenosine diphosphate
AMP	adenosine monophosphate
ATP	adenosine triphosphate
CoA	coenzyme A
COPASI	Complex Pathway Simulator
DMAPP	dimethylallyl diphosphate
ESI	electron spray ionization
FPPS	(2*E*,6*E*)-farnesyl diphosphate synthase
GDH	glucose dehydrogenase
GDL	glucono δ-lactone
Glc	glucose
HMG-CoA	3-hydroxy-3-methylglutaryl-CoA
HMGR	3-hydroxy-3-methylglutaryl-coenzyme A reductase
HMGS	3-hydroxy-3-methylglutaryl-CoA synthase
IDI	isopentenyl diphosphate δ-isomerase
LC-MS	liquid chromatography-mass spectrometry
MDC	diphosphomevalonate decarboxylase
MVK	mevalonate kinase
NADP(H)	nicotinamide adenine dinucleotide phosphate
PMK	phosphomevalonate kinase
SIM	selected ion monitoring

References

[1] K. Rosenthal, S. Lütz, *Curr. Opin. Green Sustainable Chem.* **2018**, *11*, 58–64. DOI: https://doi.org/10.1016/j.cogsc.2018.03.015

[2] M. A. Huffman et al., *Science* **2019**, *366 (6470)*, 1255–1259. DOI: https://doi.org/10.1126/science.aay8484

[3] M. A. Valliere, T. P. Korman, M. A. Arbing, J. U. Bowie, *Nat. Chem. Biol.* **2020**, *16 (12)*, 1427–1433. DOI: https://doi.org/10.1038/s41589-020-0631-9

[4] U. Kragl, W. Kruse, W. Hummel, C. Wandrey, *Biotechnol. Bioeng.* **1996**, *52 (2)*, 309–319. DOI: https://doi.org/10.1002/(SICI)1097-0290(19961020)52:2<309::AID-BIT11>3.0.CO;2-E

[5] R. Siedentop, C. Claaßen, D. Rother, S. Lütz, K. Rosenthal, *Catalysts* **2021**, *11 (10)*, 1183. DOI: https://doi.org/10.3390/catal11101183

[6] B. H. Chen, A. Sayar, U. Kaulmann, P. A. Dalby, J. M. Ward, J. M. Woodley, *Biocatal. Biotransform.* **2006**, *24 (6)*, 449–457. DOI: https://doi.org/10.1080/10242420601068668

[7] L. Shen et al., *Nat. Commun.* **2020**, *11 (1)*, 1098. DOI: https://doi.org/10.1038/s41467-020-14830-y

[8] C. Zhong, P. Wei, Y.-H. P. Zhang, *Chem. Eng. Sci.* **2017**, *161*, 159–166. DOI: https://doi.org/10.1016/j.ces.2016.11.047

[9] M. Dirkmann, J. Nowack, F. Schulz, *ChemBioChem* **2018**, *19 (20)*, 2146–2151. DOI: https://doi.org/10.1002/cbic.201800128

[10] S. Hoops, R. Gauges, C. Lee, J. Pahle, N. Simus, M. Singhal, L. Xu, P. Mendes, U. Kummer, *Bioinformatics* **2006**, *22 (24)*, 3067–3074. DOI: https://doi.org/10.1093/bioinformatics/btl485

[11] https://copasi.org (Accessed on August 09, 2022)

[12] M. Becker, P. Nikel, J. N. Andexer, S. Lütz, K. Rosenthal, *Biomolecules* **2021**, *11 (4)*, 590. DOI: https://doi.org/10.3390/biom11040590

[13] T. P. Korman, P. H. Opgenorth, J. U. Bowie, *Nat. Commun.* **2017**, *8 (1)*, 15526. DOI: https://doi.org/10.1038/ncomms15526

[14] S. Mordhorst, J. Siegrist, M. Müller, M. Richter, J. N. Andexer, *Angew. Chem., Int. Ed.* **2017**, *56 (14)*, 4037–4041. DOI: https://doi.org/10.1002/anie.201611038

[15] C. J. Thibodeaux, H. Liu, *Arch. Biochem. Biophys.* **2017**, *632*, 47–58. DOI: https://doi.org/10.1016/j.abb.2017.05.017

[16] V. Durbecq, G. Sainz, Y. Oudjama, B. Clantin, C. Bompard-Gilles, C. Tricot, J. Caillet, V. Stalon, L. Droogmans, V. Villeret, *EMBO J.* **2001**, *20 (7)*, 1530–1537. DOI: https://doi.org/10.1093/emboj/20.7.1530

[17] S. C. Rothman, T. R. Helm, C. D. Poulter, *Biochemistry* **2007**, *46 (18)*, 5437–5445. DOI: https://doi.org/10.1021/bi0616347

[18] J. Rolf, M. K. Julsing, K. Rosenthal, S. Lütz, *Molecules* **2020**, *25 (8)*, 1881. DOI: https://doi.org/10.3390/molecules25081881

[19] R. Siedentop, K. Rosenthal, *Int. J. Mol. Sci.* **2022**, *23 (7)*, 3605. DOI: https://doi.org/10.3390/ijms23073605

[20] www.brenda-enzymes.org (Accessed on August 09, 2022)

[21] A. S. Reger, J. M. Carney, A. M. Gulick, *Biochemistry* **2007**, *46 (22)*, 6536–6546. DOI: https://doi.org/10.1021/bi6026506

[22] A. B. Hawkins, M. W. W. Adams, R. M. Kelly, *Appl. Environ. Microbiol.* **2014**, *80 (8)*, 2536–2545. DOI: https://doi.org/10.1128/AEM.04146-13

[23] A. Sutherlin, M. Hedl, B. Sanchez-Neri, J. W. Burgner, C. V. Stauffacher, V. W. Rodwell, *J. Bacteriol.* **2002**, *184 (15)*, 4065–4070. DOI: https://doi.org/10.1128/JB.184.15.4065-4070.2002

[24] D.-Y. Kim, C. V. Stauffacher, V. W. Rodwell, *Biochemistry* **2000**, *39 (9)*, 2269–2275. DOI: https://doi.org/10.1021/bi991749t

[25] Y. A. Primak, M. Du, M. C. Miller, D. H. Wells, A. T. Nielsen, W. Weyler, Z. Q. Beck, *Appl. Environ. Microbiol.* **2011**, *77 (21)*, 7772–7778. DOI: https://doi.org/10.1128/AEM.05761-11

[26] S. S. Doun, J. W. Burgner, S. D. Briggs, V. W. Rodwell, *Protein Sci.* **2005**, *14 (5)*, 1134–1139. DOI: https://doi.org/10.1110/ps.041210405

[27] D. V. Krepkiy, H. M. Miziorko, *Biochemistry* **2005**, *44 (7)*, 2671–2677. DOI: https://doi.org/10.1021/bi0484217

[28] T. Koyama, S. Obata, K. Saito, A. Takeshita-Koike, K. Ogura, *Biochemistry* **1994**, *33 (42)*, 12644–12648. DOI: https://doi.org/10.1021/bi00208a015

